ACS APPLIED MATERIALS & INTERFACES

RESEARCH ARTICLE

www.acsami.org

Synthesis and Photoluminescent Properties of $(La,Ca)_3Si_6N_{11}:Ce^{3+}$ Fine Powder Phosphors for Solid-State Lighting

Takayuki Suehiro*

Institute of Multidisciplinary Research for Advanced Materials, Tohoku University, 2-1-1 Katahira, Aoba-ku, Sendai 980-8577, Japan

Naoto Hirosaki and Rong-Jun Xie

Nano Ceramics Center, National Institute for Materials Science, 1-1 Namiki, Tsukuba 305-0044, Japan

ABSTRACT: We have developed a new Ce^{3+}-activated nitride phosphor, $(La,Ca)_3Si_6N_{11}:Ce^{3+}$, using the gas-reduction−nitridation method. The synthesized $(La,Ca)_3Si_6N_{11}:Ce^{3+}$ possesses tunable yellow broadband emission with the dominant wavelength of 577−581 nm and the external quantum efficiency up to ∼42%, under an excitation of 450 nm. Precise steady-state and time-resolved photoluminescence analyses revealed that the only one type of Ce^{3+} center is active under the blue-light excitation. By combining the synthesized $(La,Ca)_3Si_6N_{11}:Ce^{3+}$ phosphors with the 450-nm InGaN chip, a broad range of white light with the correlated color temperatures of ∼2600−3800 K can be created, demonstrating their promising applicability to the warm-white light-emitting diodes.

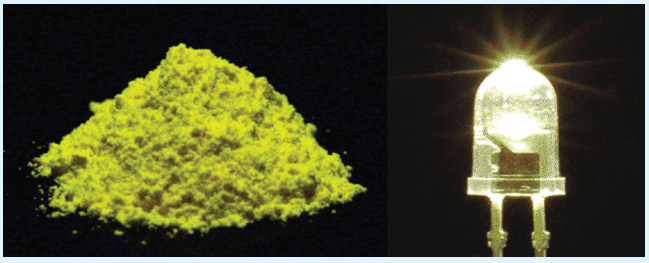

KEYWORDS: nitride, phosphor, photoluminescence, white LEDs, solid-state lighting

1. INTRODUCTION

White light-emitting diodes (LEDs) have been attracting increased attention as a light source for the next-generation general illumination and the automotive lighting applications, because of the energy savings and positive environmental effects promised by the solid-state lighting.[1−4] Currently, the most common approach for manufacturing white LEDs is to use a yellow-emitting $(Y,Gd)_3(Al,Ga)_5O_{12}:Ce^{3+}$ ($YAG:Ce^{3+}$) phosphor with a blue InGaN LED chip, by which only a cool-white light with high correlated color temperatures (CCTs) of ∼4500−6500 K can be created. The lower color temperatures required for several important applications, e.g., residential and commercial lighting, have been attained by the recent developments of the blue-light excitable and orangish-yellow- to red-emitting nitride phosphors, such as $Sr_2Si_5N_8:Eu^{2+}$,[5,6] Ca-α-SiAlON:Eu^{2+},[7,8] and $CaAlSiN_3:Eu^{2+}$.[9,10] Sakuma et al.[11] have reported the fabrication of blue InGaN-based, single phosphor-converted (1-pc) warm-white LED using the Ca-α-SiAlON:Eu^{2+} orangish-yellow phosphor, and the attained low CCT of 2750 K with the luminous efficacy of 25.9 lm/W and the general color rendering index (CRI) Ra value of 57. More recently, Li et al.[12] succeeded in realizing the 1-pc warm-white LEDs, using orangish-yellow-emitting Ce^{3+}-doped $CaAlSiN_3$ phosphors covering the CCT of ∼3500−3700 K with the luminous efficacy of 47−50 lm/W and the Ra value of ∼70. Note that, so far, the luminescent properties competing with $YAG:Ce^{3+}$ have been achieved by only a few Ce^{3+}-activated phosphors, such as $CaAlSiN_3:Ce^{3+}$ (ref 12) and $LaSr_2AlO_5:Ce^{3+}$ (refs 13 and 14) with a practically high quantum efficiency and reproducibility, in contrast to the numerous developments of the Eu^{2+}-activated yellow- to red-emitting LED phosphors.[5−10,15−17] In this work, we synthesized the new orangish-yellow-emitting nitride phosphor, $(La,Ca)_3Si_6N_{11}:Ce^{3+}$ from the $La_2O_3−CaO−CeO_2−SiO_2$ system, using the gas-reduction−nitridation (GRN) method,[18−24] and explored its potentiality as a wavelength-conversion phosphor for warm-white LEDs.

2. EXPERIMENTAL SECTION

2.1. Powder Synthesis by GRN. The powder samples with the nominal composition $(La_{1-x-y}Ca_xCe_y)_3Si_6O_{3x}N_{11-3x}$ were synthesized using the GRN method.[18−24] The oxide starting materials were prepared by simple wet mixing of $La(NO_3)_3·6H_2O$ (Wako Pure Chemical Industries, Ltd., 99.9%), $Ca(NO_3)_2·4H_2O$ (Wako Pure Chemical Industries, Ltd., 99.9%), CeO_2 (NanoTek, Kanto Chemical Co., 99.5%) and SiO_2 (SP-03B, Fuso Chemical Co.) powders, with subsequent drying at 450 °C for 2 h in air. The raw powders thus obtained were first heated at 1300 °C for 4 h in a flowing NH_3−1.0 vol % CH_4 gas mixture, followed by the second-step heating at 1450 °C for 1 h ($y = 0.20$) or 0.5 h ($y = 0.50$) in an NH_3−0.5 vol % CH_4. An additional post-synthesis heat treatment was conducted at 1500 °C for 12 h in a N_2 atmosphere.

2.2. Characterization. Physicochemical properties of the synthesized powders were characterized by X-ray diffractometry (XRD), using Cu Kα radiation (Model RINT2200, Rigaku), quantitative nitrogen/

Received: November 25, 2010
Accepted: February 10, 2011
Published: March 03, 2011

Table 1. Physicochemical Properties of $(La_{1-x-y}Ca_xCe_y)_3Si_6N_{11}$ Powders Synthesized by the GRN

	Composition					
sample	x	y	purity[a] (wt %)	lattice volume ($\times 10^6$ pm^3)	C_N (wt %)	C_O (wt %)
20	0.00	0.20			20.4(1)	1.24(1)
C20	0.05	0.20	65	500.14(1)	20.7(1)	1.23(1)
50	0.00	0.50	80	498.51(1)	20.4(1)	1.19(1)
C50	0.05	0.50	78	498.12(1)	20.7(1)	1.39(1)

[a] Determined by the Rietveld analysis.

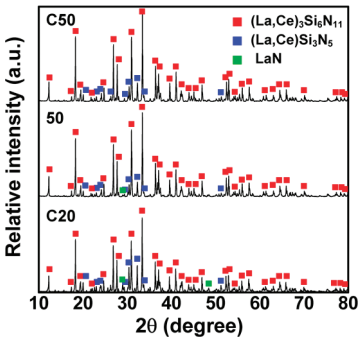

Figure 1. XRD patterns of the synthesized $(La,Ca)_3Si_6N_{11}:Ce^{3+}$ powders.

oxygen analysis (Model TC-436, LECO Co.), and surface area measurement (Model ASAP2020, Shimadzu). Photoluminescence (PL) spectra and quantum efficiencies were measured at room temperature, using a spectrofluorometer equipped with a 60-mm integrating sphere (FP-6500/ISF-513, Jasco). The spectral bandwidth (resolution) was 1 nm on both the excitation and emission monochromators. Quantum efficiencies were calculated according to the equation described elsewhere,[25] which leads to the relationship $QE_{ext} = \alpha QE_{int}$, where α is the absorption, QE_{ext} the external quantum efficiency, and QE_{int} the internal quantum efficiency. Time-resolved PL measurements were conducted using a time-correlated single-photon counting fluorometer (Tempro, Horiba Jobin−Yvon) equipped with LED excitation sources of 455 and 493 nm with the pulse duration full width at half-maximum (fwhm) of ∼1 ns. The emission was filtered through a narrow-band (∼9 nm) interference filter of 620 nm, and the instrumental response function (IRF) was obtained by measuring a Ludox colloidal silica suspension. Temperature-dependent PL properties were measured at an excitation wavelength of 450 nm, using a multichannel spectrometer (Model MCPD-7000, Otsuka Electronics). The prototype 1-pc-converted white LEDs were fabricated using the as-prepared $(La,Ca)_3Si_6N_{11}:Ce^{3+}$ powders with a 450-nm InGaN blue LED die (wall plug efficiency of ∼22%).

3. RESULTS AND DISCUSSION

3.1. GRN Synthesis and Characterization. Main physicochemical properties of the synthesized $(La,Ca)_3Si_6N_{11}:Ce^{3+}$ powders are summarized in Table 1, and their XRD patterns are shown in Figure 1. It was found from the preliminary experiments that the samples prepared with the compositions $x = 0$ and $y < 0.20$ showed significant disproportionation into the $(La,Ce)Si_3N_5$ and LaN (with the lattice constant of 530.62(3) pm) phases, while the $(La,Ce)_3Si_6N_{11}$ phase hardly formed. The addition of a small amount (5 mol %) of calcium was found to effectively promote the liquid-assisted homogenization of the reaction system, enabling the formation of $(La,Ce)_3Si_6N_{11}$ phase in 65% phase purity for $y = 0.20$ (sample C20). This is

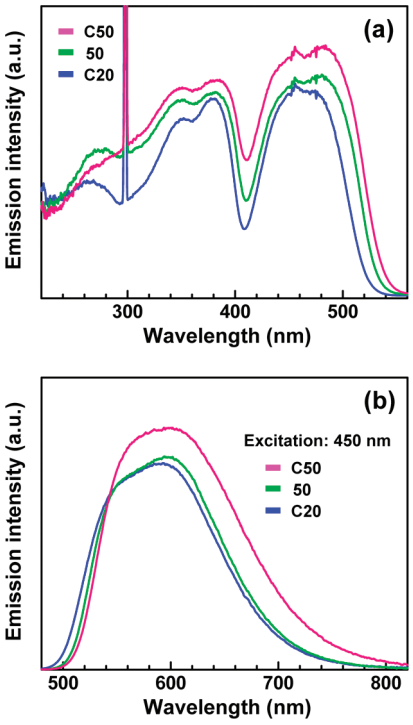

Figure 2. Photoluminiscence (PL) (a) excitation and (b) emission spectra of the synthesized $(La,Ca)_3Si_6N_{11}:Ce^{3+}$ samples. The sharp lines in excitation spectra are due to an experimental artifact (half order of the monitoring wavelength).

attributable to the much-lower eutectic temperature of the $CaO-SiO_2$ system,[26] viz, 1436 °C, compared to 1625 °C in the $La_2O_3-SiO_2$ system.[27] The appreciable lattice shrinkages were observed with the addition of calcium or an increase in the Ce concentration, indicative of the substitution of smaller Ca^{2+} (112 pm, 8CN) and Ce^{3+} (114.3 pm) for La^{3+} ion (116.0 pm).[28] The crystal structure of $(La,Ca)_3Si_6N_{11}:Ce^{3+}$ belongs to the tetragonal space group *P4bm*, in which Ce^{3+} can occupy two different La^{3+} sites with the 8-fold coordination of nitrogen.[29,30] The La1 (4c) site forms a distorted bicapped trigonal prism with the average La−N bond distance of ∼270 pm, while the La2 (2a) site forms a square antiprism with the average La−N distance of ∼262 pm. From the preliminary Rietveld refinement of the occupation factors of La^{3+} for sample C50, the actual solubility of calcium was estimated to be 0.162(9) and 0.154(10) for the La1 and La2 sites, respectively, giving the overall composition of $(La_{0.340(9)}Ca_{0.160(9)}Ce_{0.500})_3Si_6O_{0.48(3)}N_{10.52(3)}$. The analyzed nitrogen contents (C_N) were found to be comparable to the nominal values (20.8−20.9 wt %) in every sample, indicating the complete nitridation. The impurity oxygen content (C_O) was

Table 2. Photoluminescent Properties of the Synthesized $(La,Ca)_3Si_6N_{11}:Ce^{3+}$ Samples under Excitation at 450 nm

	CIE Coordination					Quantum Efficiencies (%)		
sample	x	y	λ_d (nm)	λ_{p1} (nm)	λ_{p2} (nm)	Abs	IQE	EQE
C20	0.487	0.502	576.9	537	596	83.6	38.5	32.2
50	0.501	0.492	578.7	541	599	86.0	37.7	32.4
C50	0.517	0.478	581.0	554	608	87.1	48.6	42.4

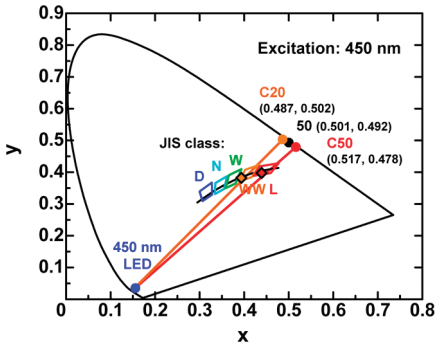

Figure 3. CIE1931 chromaticity coordinates of the synthesized $(La,Ca)_3Si_6N_{11}:Ce^{3+}$ phosphors. The chromaticity coordinates of the fabricated white LEDs are also indicated.

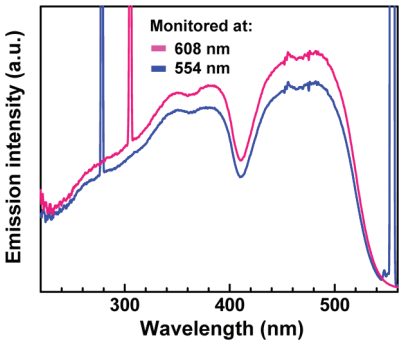

Figure 4. PL excitation spectra for the sample C50, measured with the monitoring wavelength of λ_{p1} = 554 nm and λ_{p2} = 608 nm.

maintained as low as 1.19−1.39 wt % and was comparable to the value estimated from the Rietveld analysis (1.11 wt %), indicating that the possible cation deficiency introduced by the dissolution of impurity oxygen[31] might be effectively eliminated by the aliovalent substitution of Ca^{2+}, as revealed by the quantum efficiency measurements to be discussed later. The particle sizes estimated from the surface area measurement were determined to be 2.14−2.26 μm.

3.2. PL Excitation and Emission Properties. The PL excitation and emission spectra of the synthesized $(La,Ca)_3Si_6N_{11}:Ce^{3+}$ samples measured at room temperature are shown in Figure 2, and the relevant spectral parameters and the quantum efficiencies are listed in Table 2. The PL excitation spectra consisted of at least five broad bands with maxima at 485, 455, 385, 350, and 270 nm (for sample C50), which correspond to transitions from the Ce^{3+} 4f ($^2F_{5/2}$) ground state to the various 5d crystal-field components. The crystal-field splitting (CFS) derived from the energy difference between the observed highest and the lowest 5d level was 1.64×10^4 cm^{-1}, which is significantly larger than the value observed for $LaSi_3N_5:Ce^{3+}$ (1.10×10^4 cm^{-1}),[21] which exhibits blue emission under the UV excitation of ∼250−380 nm. The estimated 5d energy centroid was 2.88×10^4 cm^{-1}, showing a further reduction, compared to 3.37×10^4 cm^{-1} in $LaSi_3N_5:Ce^{3+}$.[21] These considerations were based on the assumption that the observed highest and lowest 5d absorption should originate from an identical Ce^{3+} center. Therefore, one cannot exclude the possibilities of overestimating the CFS, as well as underestimating the centroid shift. The obvious fact that the appreciably shorter (La,Ce)−N bond distances, compared to $LaSi_3N_5:Ce^{3+}$ with the same activator concentration (269/261 pm vs 278 pm), might lead to the stronger crystal fields, resulting in the significantly red-shifted excitation and emission properties attained in the current system. The marked reduction of the 5d centroid can be also rationalized by the relationship between the energy centroid and the effective coordination radius (i.e., R_{eff}^{-6} dependence of the centroid shift).[32] The emission spectra showed asymmetric broadband characteristics of a 5d−4f transition in Ce^{3+} with the dominant wavelength (λ_d) of 577−581 nm, giving an orangish-yellow emission. The corresponding chromaticity coordinates varied from (0.487, 0.502) for sample C20 to (0.517, 0.478) for sample C50, which enables the fabrication of bichromatic warm-white LEDs possessing broad CCT in the range of ∼3800−2600 K (see Figure 3), covering the "warm white" (Japanese Industrial Standard Z9112, class WW) to the "incandescent lamp color" (class L). The fwhm of the emission spectrum ranged from 130 nm to 143 nm, which is significantly broader than that observed for the Eu^{2+}-activated Ca-α-SiAlON (∼95 nm) with the similar chromaticity.[20] The fwhm values amount to $3.76-3.96 \times 10^3$ cm^{-1}, which is comparable to that typically observed for Ce^{3+}-activated phosphors containing a single type of luminescent center (∼4×10^3 cm^{-1}).[33] For every sample, the emission spectrum could be deconvoluted into two Gaussian components, centered at λ_{p1} (higher-energy side) and λ_{p2} (lower-energy side) in an energy scale. The energy difference of the two bands was in the range of $(1.62-1.85) \times 10^3$ cm^{-1}, which is consistent with the values reported earlier;[12,14,21,33] these were ascribed to the splitting of the $^2F_{7/2,5/2}$ ground state. The excitation spectra showed no detectable changes at the two different monitoring wavelengths of λ_{p1} and λ_{p2} (see Figure 4), indicating that the two emission bands resulted from the identical luminescent center. The above luminescent characteristics conclusively showed that only one type of Ce^{3+} center contributes to the observed yellow emission under the blue-light excitation, as will be revealed by the time-resolved PL measurements discussed below.

3.3. Time-Resolved PL Properties. The analyzed PL decay rates (τ) for the synthesized $(La,Ca)_3Si_6N_{11}:Ce^{3+}$ samples are summarized in Table 3, and the decay curves for the sample C20 are shown in Figure 5. The luminescence decay measurement was conducted under the excitation wavelengths of 455 and 493 nm, which correspond closely to the observed two lowest 5d absorption bands in the excitation spectra (see Figure 2a). The

Table 3. Analyzed Decay Rates for the Emission of 620 nm under Excitation at 493 and 455 nm

sample	τ_{493} (ns)	τ_{455} (ns)
C20	41.79(12)	42.34(12)
50	42.16(9)	42.29(10)
C50	41.94(8)	42.11(9)

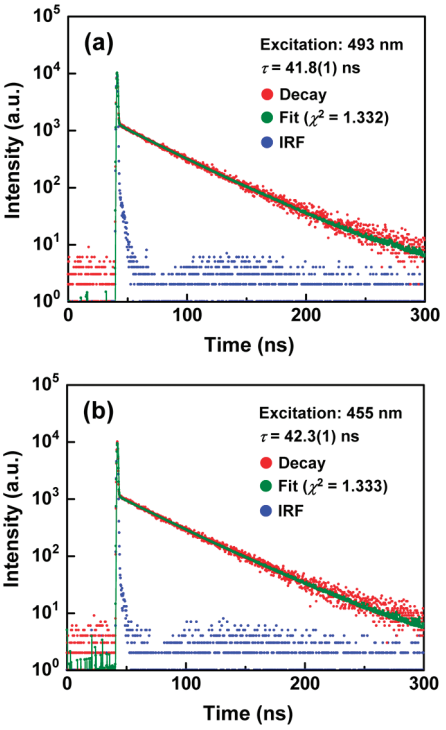

Figure 5. PL decay curves for sample C20 under excitation at (a) 493 nm and (b) 455 nm.

above excitation and the monitoring conditions (~620 nm) completely eliminated the influence of blue emission from the $(La,Ce)Si_3N_5$ secondary phase. The decay profiles showed an obvious single-exponential behavior ($I/I_0 = \exp(-t/\tau)$[34]) in every case for both excitation conditions with a short decay time of ~42 ns, which corresponds to the value typically observed for the allowed 5d−4f transition in Ce^{3+} (~20−60 ns).[35] The consistency in the decay time among the samples implies a saturated energy transfer among Ce^{3+} centers, reflecting the high activator concentration of the present compositions. These results, as well as the steady-state PL properties previously discussed, clearly indicated that the observed yellow emission under the blue-light excitation originated from the 5d−4f transition in a single type of Ce^{3+} center, which possesses the lower-lying 5d energy levels between the aforementioned two different Ce^{3+} sites. The possibilities of some site preference of Ce^{3+} and/or the occurrence of an energy transfer from the Ce^{3+} center possessing higher-lying 5d levels will be further examined in our future studies, with regard to the results for single-phase samples.

3.4. Quantum Efficiencies. As seen in Table 2, samples 50 and C50 with the identical activator concentration possessed comparably high absorption efficiency (Abs) values of ~86%−87%, while sample C50 exhibited the markedly higher external

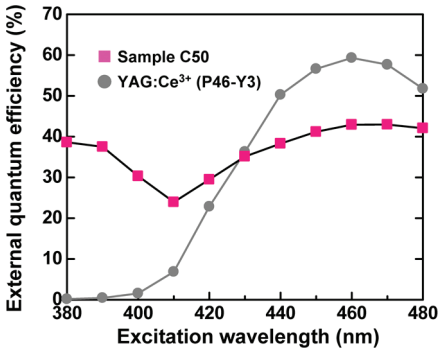

Figure 6. Dependence of the external quantum efficiency (EQE) on the excitation wavelength for sample C50.

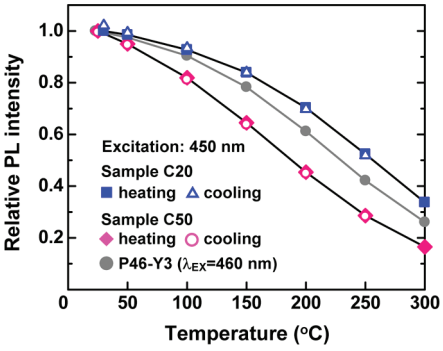

Figure 7. Temperature dependence of the PL intensity for samples C20 and C50.

quantum efficiency (EQE) of 42.4%, compared to 32.4% in sample 50. This resulted from the significant improvement of the internal quantum efficiency (IQE) in the Ca-containing sample (C50), indicating that the impurity oxygen-induced lattice defects (i.e., possible cation vacancies) might be decreased by the compensating substitution of Ca^{2+} for La^{3+}. Sample C20 exhibited the lower EQE of 32.2%, reflecting its lower phase purity, while its apparently low IQE might result from an overestimation of the absorption, because of the inclusion of the conductive LaN secondary phase.[36] As expected from the favorable distribution of the 5d energy levels in the near-ultraviolet (near-UV) to violet region, $(La,Ca)_3Si_6N_{11}:Ce^{3+}$ possesses better flexibility to the excitation sources, in contrast to $YAG:Ce^{3+}$, and sample C50 indeed exhibited higher EQE values than the commercial $YAG:Ce^{3+}$ phosphor (P46−Y3) under an excitation of <430 nm (see Figure 6).

3.5. Temperature-Dependent PL Properties. Figure 7 shows the temperature dependence of the PL intensity for samples C20 and C50, together with that of the commercial $YAG:Ce^{3+}$ phosphor, for comparison. Sample C50 showed a relatively low quenching temperature (T_{50} = 188 °C), mainly because of its high activator concentration, whereas sample C20 showed better thermal stability (T_{50} = 257 °C), compared to $YAG:Ce^{3+}$ (T_{50} = 229 °C), indicating the intrinsically high thermal stability of $(La,Ca)_3Si_6N_{11}:Ce^{3+}$. The PL intensity of sample C20 at 150 °C retained 84% of the intensity measured at room temperature, which matches well with the temperature dependencies of most of the nitride LED phosphors.[15,31,37] The emission profile showed no discernible changes upon increasing temperature (see Figure 8), as proven by the minimal chromaticity variation between 30 °C to 200 °C, being as small as 0.008

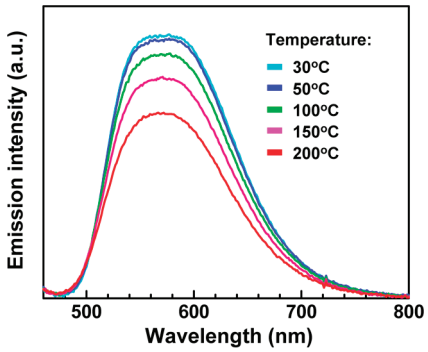

Figure 8. PL emission spectra of sample C20, measured at various temperature with an excitation wavelength of 450 nm.

Table 4. Optical Properties of the White LEDs Fabricated Using the $(La,Ca)_3Si_6N_{11}:Ce^{3+}$ Phosphors

	CIE Coordination					
phosphor used	*x*	*y*	CCT (K)	Ra	JIS class	η^a (lm/W)
C20	0.394	0.382	3704	69	WW	34.3
C50	0.439	0.398	2911	65	L	34.8

[a] Luminous efficacy.

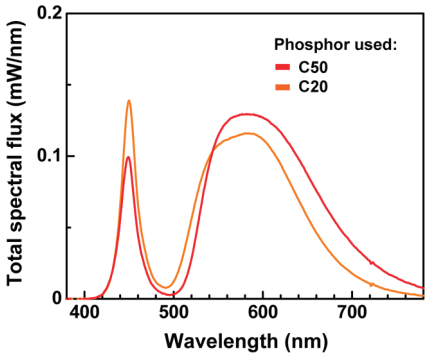

Figure 9. Emission spectra of the white LEDs fabricated using the synthesized $(La,Ca)_3Si_6N_{11}:Ce^{3+}$ phosphors.

for sample C20. The compositional optimization of the samples (i.e., lower Ce concentration with an appropriate doping of calcium) will enable further improvement of the thermal stability, while maintaining the effectively red-shifted emission.

3.6. Application to Warm-White LEDs. We fabricated the prototype 1-pc-white LED devices by combining the synthesized samples C20 and C50 with a 450-nm InGaN blue LED die. The optical properties of the fabricated white LEDs are summarized in Table 4, and their emission spectra are shown in Figure 9. Warm-white lights with CCTs of 3704 K (class WW) and 2911 K (class L) could be successfully created with samples C20 and C50, respectively, because of the composition-tunable emission properties of $(La,Ca)_3Si_6N_{11}:Ce^{3+}$. The CRI Ra value was moderately high for a low-CCT bichromatic system, in the range of 65−69, which was comparable to that attained by $CaAlSiN_3:Ce^{3+}$,[12] while showing much improvement compared to the system using Ca-α-SiAlON:Eu^{2+} with the similar CCT of 2750−2700 K.[9,11] Although sample C20 possessed the lower EQE, its shorter emission wavelength and higher thermal stability resulted in the comparable luminous efficacy of both assembled LEDs being ∼35 lm/W, under a forward-bias current of 20 mA.

4. CONCLUSIONS

We have synthesized a new orangish-yellow-emitting phosphor, $(La,Ca)_3Si_6N_{11}:Ce^{3+}$, via a simple and facile gas-reduction−nitridation method. The synthesized $(La,Ca)_3Si_6N_{11}:Ce^{3+}$ possessed external quantum efficiency (EQE) values up to ∼42% under the blue-light excitation, as well as the potentially high thermal stability, compared to YAG:Ce^{3+}, even under the tentatively optimized processing conditions. Both steady-state and time-resolved photoluminescence (PL) analyses clearly indicated that only one type of Ce^{3+} center possessing lower-lying 5d levels contributes to the observed yellow emission under the blue-light excitation. By combining the synthesized $(La,Ca)_3Si_6N_{11}:Ce^{3+}$ phosphors with the blue InGaN LED chip, a broad range of warm-white lights with CCTs of 2911 and 3704 K have been created, along with better CRI Ra values, compared to the existing Eu^{2+}-activated yellow-emitting phosphors.

AUTHOR INFORMATION

Corresponding Author

*E-mail: suehiro@tagen.tohoku.ac.jp.

ACKNOWLEDGMENT

We are grateful to Mr. Y. Yajima and Ms. K. Nakajima of National Institute for Materials Science for their valuable cooperation. T.S. acknowledges Professor T. Sato of IMRAM, Tohoku University, for fruitful discussions.

REFERENCES

(1) Schubert, E. F.; Kim, J.-K. *Science* **2005**, *308*, 1274.
(2) Shur, M. S.; Žukauskas, A. *Proc. IEEE* **2005**, *93*, 1691.
(3) Narukawa, Y.; Narita, J.; Sakamoto, T.; Yamada, T.; Narimatsu, H.; Sano, M.; Mukai, T. *Phys. Status Solidi A* **2007**, *204*, 2087.
(4) Tsao, J. Y.; Coltrin, M. E.; Crawford, M. H.; Simmons, J. A. *Proc. IEEE* **2010**, *98*, 1162.
(5) Mueller-Mach, R.; Mueller, G.; Krames, M. R.; Höppe, H. A.; Stadler, F.; Schnick, W.; Juestel, T.; Schmidt, P. *Phys. Status Solidi A* **2005**, *202*, 1727.
(6) Li, Y. Q.; van Steen, J. E. J.; van Krevel, J. W. H.; Botty, G.; Delsing, A. C. A.; DiSalvo, F. J.; de With, G.; Hintzen, H. T. *J. Alloys Compd.* **2006**, *417*, 273.
(7) Xie, R.-J.; Hirosaki, N.; Sakuma, K.; Yamamoto, Y.; Mitomo, M. *Appl. Phys. Lett.* **2004**, *84*, 5404.
(8) Xie, R.-J.; Hirosaki, N.; Mitomo, M.; Yamamoto, Y.; Suehiro, T.; Sakuma, K. *J. Phys. Chem. B* **2004**, *108*, 12027.
(9) Sakuma, K.; Hirosaki, N.; Kimura, N.; Ohashi, M.; Xie, R.-J.; Yamamoto, Y.; Suehiro, T.; Asano, K.; Tanaka, D. *IEICE Trans. Electron.* **2005**, *E88-C*, 2057.
(10) Uheda, K.; Hirosaki, N.; Yamamoto, Y.; Naito, A.; Nakajima, T.; Yamamoto, H. *Electrochem. Solid State Lett.* **2006**, *9*, H22.
(11) Sakuma, K.; Omichi, K.; Kimura, N.; Ohashi, M.; Tanaka, D.; Hirosaki, N.; Yamamoto, Y.; Xie, R. J.; Suehiro, T. *Opt. Lett.* **2004**, *29*, 2001.
(12) Li, Y. Q.; Hirosaki, N.; Xie, R.-J.; Takeda, T.; Mitomo, M. *Chem. Mater.* **2008**, *20*, 6704.
(13) Im, W. B.; Kim, Y.-I.; Fellows, N. N.; Masui, H.; Hirata, G. A.; DenBaars, S. P.; Seshadri, R. *Appl. Phys. Lett.* **2008**, *93*, 091905.
(14) Im, W. B.; Fellows, N. N.; DenBaars, S. P.; Seshadri, R.; Kim, Y.-I. *Chem. Mater.* **2009**, *21*, 2957.

(15) Xie, R. J.; Hirosaki, N. *Sci. Technol. Adv. Mater.* **2007**, *8*, 588.
(16) Park, J. K.; Kim, C. H.; Park, S. H.; Park, H. D.; Choi, S. Y. *Appl. Phys. Lett.* **2004**, *84*, 1647.
(17) Pardha, M.; Varadaraju, U. V. *Chem. Mater.* **2006**, *18*, 5267.
(18) Suehiro, T.; Hirosaki, N.; Komeya, K. *Nanotechnology* **2003**, *14*, 487.
(19) Suehiro, T.; Hirosaki, N.; Xie, R.-J.; Mitomo, M. *Chem. Mater.* **2005**, *17*, 308.
(20) Suehiro, T.; Hirosaki, N.; Xie, R.-J.; Sakuma, K.; Mitomo, M.; Ibukiyama, M.; Yamada, S. *Appl. Phys. Lett.* **2008**, *92*, 191904.
(21) Suehiro, T.; Hirosaki, N.; Xie, R.-J.; Sato, T. *Appl. Phys. Lett.* **2009**, *95*, 051903.
(22) Suehiro, T.; Onuma, H.; Hirosaki, N.; Xie, R.-J.; Sato, T.; Miyamoto, A. *J. Phys. Chem. C* **2010**, *114*, 1337.
(23) Hirosaki, N.; Suehiro, T. U.S. Patent 7598194 B2, 2009.
(24) Hirosaki, N.; Suehiro, T. Chin. Patent ZL 2005800090952, 2009.
(25) Hirosaki, N.; Xie, R.-J.; Kimoto, K.; Sekiguchi, T.; Yamamoto, Y.; Suehiro, T.; Mitomo, M. *Appl. Phys. Lett.* **2005**, *86*, 211905.
(26) Pelton, A. D.; Blander, M. *Metall. Trans. B* **1986**, *17B*, 805.
(27) Toropov, N. A.; Bondar, I. A. *Izv. Akad. Nauk SSSR, Otd. Khim. Nauk* **1961**, *5*, 740.
(28) Shannon, R. D. *Acta Crystallogr., Sect. A: Cryst. Phys., Diffr., Theor. Gen. Crystallogr.* **1976**, *32*, 751.
(29) Woike, M.; Jeitschko, W. *Inorg. Chem.* **1995**, *34*, 5105.
(30) Schlieper, T.; Schnick, W. *Z. Anorg. Allg. Chem.* **1995**, *621*, 1535.
(31) Xie, R.-J.; Hirosaki, N.; Suehiro, T.; Xu, F.-F.; Mitomo, M. *Chem. Mater.* **2006**, *18*, 5578.
(32) Dorenbos, P. *Phys. Rev. B* **2000**, *62*, 15640.
(33) Blasse, G.; Bril, A. *J. Chem. Phys.* **1967**, *47*, 5139.
(34) I and I_0 are the luminescence intensities at time t and 0, respectively; τ is the decay time.
(35) Lin, H.; Liang, H.; Han, B.; Zhong, J.; Su, Q.; Dorenbos, P.; Birowosuto, M. D.; Zhang, G.; Fu, Y.; Wu, W. *Phys. Rev. B* **2007**, *76*, 035117.
(36) Didchenko, R.; Gortsema, F. P. *J. Phys. Chem. Solids* **1963**, *24*, 863.
(37) Xie, R.-J.; Hirosaki, N.; Li, H.-L.; Li, Y. Q.; Mitomo, M. *J. Electrochem. Soc.* **2007**, *154*, J314.